

Title: A Computational Comparison of High Strain Rate Strength and Failure Models for Glass

Authors: Timothy G. Talladay
Douglas W. Templeton

¹US Army Tank-Automotive Research, Development, and Engineering Center,
6501 E. 11 Mile Rd, Warren, MI 48397, USA

Paper ID: 13963473

Report Documentation Page				Form Approved OMB No. 0704-0188	
Public reporting burden for the collection of information is estimated to average 1 hour per response, including the time for reviewing instructions, searching existing data sources, gathering and maintaining the data needed, and completing and reviewing the collection of information. Send comments regarding this burden estimate or any other aspect of this collection of information, including suggestions for reducing this burden, to Washington Headquarters Services, Directorate for Information Operations and Reports, 1215 Jefferson Davis Highway, Suite 1204, Arlington VA 22202-4302. Respondents should be aware that notwithstanding any other provision of law, no person shall be subject to a penalty for failing to comply with a collection of information if it does not display a currently valid OMB control number.					
1. REPORT DATE 05 NOV 2012		2. REPORT TYPE Journal Article		3. DATES COVERED 05-04-2012 to 06-08-2012	
4. TITLE AND SUBTITLE A Computational Comparison of High Strain Rate Strength and Failure Models for Glass				5a. CONTRACT NUMBER	
				5b. GRANT NUMBER	
				5c. PROGRAM ELEMENT NUMBER	
6. AUTHOR(S) Timothy Talladay; Douglas Templeton				5d. PROJECT NUMBER	
				5e. TASK NUMBER	
				5f. WORK UNIT NUMBER	
7. PERFORMING ORGANIZATION NAME(S) AND ADDRESS(ES) U.S. Army TARDEC, 6501 East Eleven Mile Rd, Warren, Mi, 48397-5000				8. PERFORMING ORGANIZATION REPORT NUMBER #23478	
9. SPONSORING/MONITORING AGENCY NAME(S) AND ADDRESS(ES) U.S. Army TARDEC, 6501 East Eleven Mile Rd, Warren, Mi, 48397-5000				10. SPONSOR/MONITOR'S ACRONYM(S) TARDEC	
				11. SPONSOR/MONITOR'S REPORT NUMBER(S) #23478	
12. DISTRIBUTION/AVAILABILITY STATEMENT Approved for public release; distribution unlimited					
13. SUPPLEMENTARY NOTES Submitted to International Symposium on Ballistics					
14. ABSTRACT Computational studies are performed using the recent Holmquist-Johnson glass model and the earlier Johnson-Holmquist brittle material model. Although the JH-2 model has been adapted to provide reasonably accurate predictions for soda-lime glass, the Holmquist-Johnson model was developed specifically to replicate the behaviors of glass. Simulations of rod impact on borosilicate glass using these two models are compared to experiments involving impact of mild steel rods and borosilicate glass at ca. 540 m/s. The material constants were adjusted to attain similar strength and damage responses at this impact velocity. In this manner, some light can be shed on the difference in the mechanisms of these two models. The models are compared and contrasted in penetration-time, penetration resistance, dwell, and the evolution of visual damage phenomena. The limitations of both models are discussed and the need for more experimental data to corroborate simulations is apparent.					
15. SUBJECT TERMS					
16. SECURITY CLASSIFICATION OF:			17. LIMITATION OF ABSTRACT Public Release	18. NUMBER OF PAGES 10	19a. NAME OF RESPONSIBLE PERSON
a. REPORT unclassified	b. ABSTRACT unclassified	c. THIS PAGE unclassified			

Computational studies are performed using the recent Holmquist-Johnson glass model and the earlier Johnson-Holmquist brittle material model. Although the JH-2 model has been adapted to provide reasonably accurate predictions for soda-lime glass, the Holmquist-Johnson model was developed specifically to replicate the behaviors of glass. Simulations of rod impact on borosilicate glass using these two models are compared to experiments involving impact of mild steel rods and borosilicate glass at *ca.* 540 m/s. The material constants were adjusted to attain similar strength and damage responses at this impact velocity. In this manner, some light can be shed on the difference in the mechanisms of these two models. The models are compared and contrasted in penetration-time, penetration resistance, dwell, and the evolution of visual damage phenomena. The limitations of both models are discussed and the need for more experimental data to corroborate simulations is apparent.

INTRODUCTION

Modeling impact on brittle materials such as ceramics and glasses has been a topic of interest for many years. Suitable material models and associated constants have been proposed by many researchers, however accuracy across a broad range of impact conditions is still not always achievable. Glasses, including soda-lime-silica and borosilicate, are widely used for protection when transparency is desired. The phenomenon of fracture, fragmentation, and total failure are complex and are still not fully understood.

In 1994, Johnson and Holmquist [1] released an improved brittle material model, hereafter referred to as the JH-2 model. This model was used successfully by a number of researchers to replicate projectile impact into glass [2 – 4]. In 2011, Holmquist and Johnson [5] developed a material model specifically for glass, hereafter referred to as the HJ model. This model better accounts for characteristics

¹ US Army Tank-Automotive Research, Development, and Engineering Center, 6501 E. 11 Mile Rd, Warren, MI 48397, USA

that are observed in glass strength, damage, and failure characteristics. This article discusses a computational comparison of the JH-2 and HJ models when applied to borosilicate glass. The computational results are compared to work by Bourne *et al.* [6, 7] and analysis by Forde *et al.* [8].

SIMULATIONS

Simulations are conducted to explore the differences between the HJ and JH-2 models for predicting the response of borosilicate glass. There are significant differences between these two models, a few characteristics are location dependent strength, variable shear modulus, and time dependent softening. The reader is encouraged to see Ref. [5] for an exhaustive list and justification for these features.

Bourne *et al.* impacted borosilicate glass with 9.5 mm diameter, hemispherical-nosed rods. The rods were 95 mm long and impacted the glass samples at 535 to 540 m/s (slightly different velocities are given in Refs. [6 – 8]). It is important to note that the four x-radiographs presented in Bourne's work are from separate experiments which were conducted approximately at the same impact conditions.

Simulations are conducted in the Lagrangian hydrocode EPIC and are run in both two-dimensional and three-dimensional axisymmetry. The impact velocity in the simulations is 537 m/s to account for the range of velocities reported in experiments. To better replicate the behavior of glass, highly distorted elements are converted to particles rather than eroded. Although computationally more intense, the flow resistance of the fragments is an important characteristic of brittle material impact resistance [9]. Both the rod and the glass are meshed with a fine, uniform, non-expanding grid. Sensitivity to mesh size is not investigated in this article. The mild steel rod is simulated with the Johnson-Cook strength and damage models, and the borosilicate glass block is modeled with the two subject brittle material models.

The material constants for borosilicate glass under the HJ model were previously derived. Constants were derived for borosilicate glass under the JH-2 model to maintain similar reference strength and failed strength profiles over the range of impact pressures which occur in this simulation. It is difficult to maintain exactly similar strength and failure profiles over a wide range of pressures due to the differences in the forms of strength models. For higher velocity impacts, it is expected that the constants used in this article for the JH-2 model would be inaccurate.

Penetration Depth

In Fig. 1, the rod nose position relative to the front face of the target is given. For the first 40 μ s, both models agree reasonably well with the experimental results. However, after 40 μ s the JH-2 simulation tracks closely with the experiment, while the HJ model significantly underpredicts the penetration. The glass block appears to be too strong in this HJ simulation. Both models and the experimental results show an increase in the rate of penetration as the glass bulk progressively fails. The point at which this change in penetration rate occurs is different between the two models. The HJ model shows a change in rate near 24 μ s, and the JH-2 model shows a more gradual change in rate from 20 to 32 μ s. The experimental results do

not appear to show a significant change in rate until 40 μ s, however there is likely some experimental error in the results because of the low number of x-ray images and the fact that the x-rays were from different impact events. Regardless, the general trend of increasing penetration rate is visible.

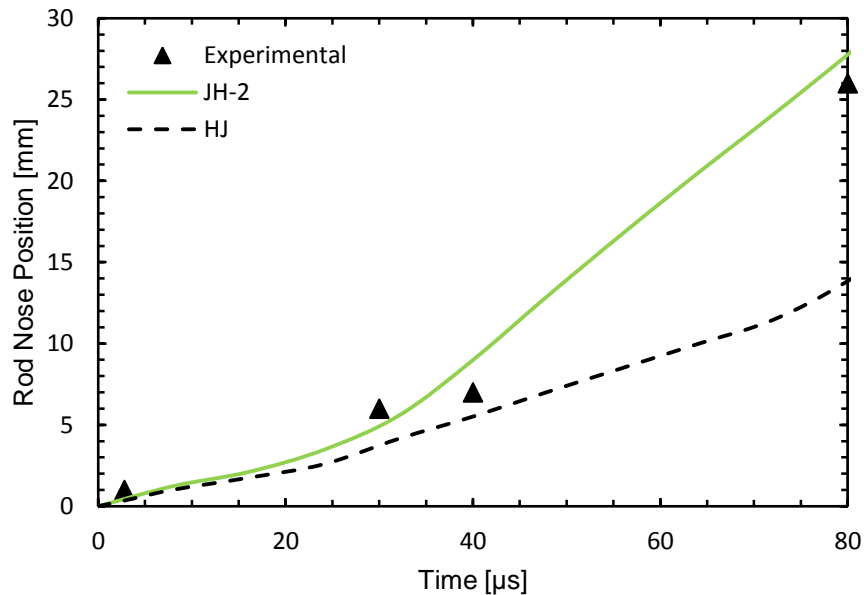


Figure 1. Rod nose position for the HJ and JH-2 models and experiment.

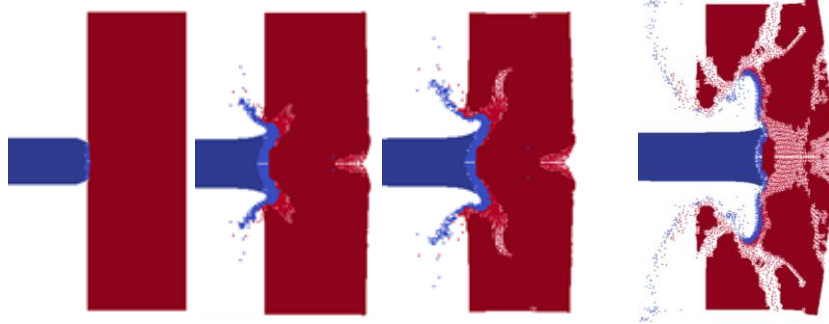
The characteristics of the nose position velocity of the two models are considerably different. Based on the simulations, the nose position (p) can be approximated as a function of time (t) by the following linear segments (time in μ s, position in mm). The first penetration rate transition in the HJ model seems to be the beginning of widespread failure in the glass block, and the second transition seems correlate to the rod sharpening effect (see Fig. 5) observed by Bourne *et al.* and the final failure of the glass. The sharpening and second transition in penetration rate are not observed in the JH-2 model.

$$\begin{aligned}
 \text{HJ Model: } & p = 0.1077t, 0 \leq t < 24 \\
 & p = 0.1845t - 1.8473, 24 \leq t < 75 \\
 & p = 0.4184t - 19.382, 75 \leq t \leq 120 \\
 \text{JH-2 Model: } & p = 0.1345t, 0 \leq t < 30 \\
 & p = 0.4461t - 9.6179, 30 \leq t \leq 120
 \end{aligned}$$

Simulations with small changes in impact velocity, less than ± 1 m/s, are also performed to determine the effect of numerical instability. The change in the calculated nose position for both models is insignificant, with variations of 1 mm or less.

A series of images of the simulation of this experiment are given in Fig. 2. The simulation images are taken at the same time as the experimental images shown in the Bourne *et al.* and Forde *et al.* articles (these images are not shown here).

HJ Model



JH-2 Model

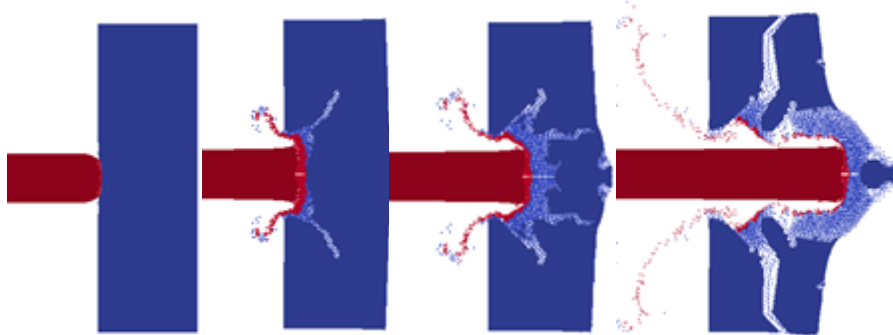


Figure 2. Series of images showing simulations of a mild steel rod impacting a 20 mm thick borosilicate glass block at 537 m/s. Images are given at 2.8, 30, 40, and 80 μ s (left to right) after impact.

At 2.8 μ s, the nose of the cylinder is deformed and has penetrated approximately 0.5 mm of the glass surface. The glass block has not yet deformed under the load of the impact. Forde *et al.* note that a cone crack appeared at this time step during the impact. They measured an approximate angle between the cone cracks of 110° . Plotting damage contours shows the formation of what appear to be cone cracks in the simulation, with an included angle of 100° in the HJ model. The JH-2 model does not appear to predict a cone crack.

For both simulations at 30 μ s, the rod has started to deform and erode, and cone cracks have started propagating into the glass block. The HJ model shows the beginning of a tensile crack opening at the rear surface, however the JH-2 model shows only deformation of the glass block. Fig. 3 shows the contours of damage (red is failed material) which may show where cracks are likely to occur, as was done by Anderson and Holmquist [10]. In this instance, both models show the general trend that is observed in the experimental image.

At 40 μ s, the penetration is substantially different between the two models. The glass cone underneath the rod is still visible in the HJ model. Rather than comminuting the material in front of the penetrator, the HJ model predicts more rod deformation/erosion, while a glass cone underneath the rod maintains substantial strength to resist penetration despite widespread material failure.

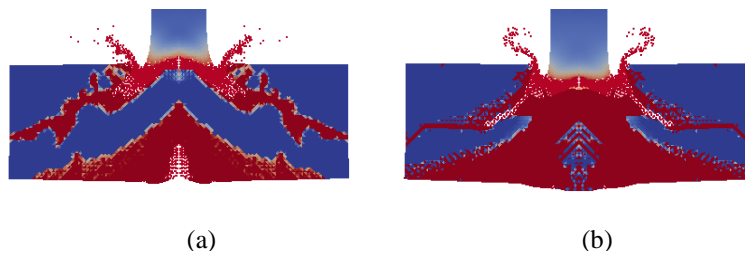


Figure 3. Contours of damage at 30 μ s for the (a) HJ model and (b) JH-2 model.

The final images in Fig. 2 show the response at 80 μ s. At this time step, the JH-2 model better replicates the penetration into the glass. In the HJ model, the glass block is still resisting penetration but moves with the rod. The approximate rod nose position from the experiment is 26 mm, and the JH-2 simulation shows an approximate nose position of 27.8 mm. The final image from the Bourne *et al.* experiment shows the deformed nose has sheared off the rod. In Fig. 4, the HJ simulation shows parts of the rod breaking off from the nose, while the JH-2 simulation does not show this breakage. From the experiment, the nose was rounded, whereas both the simulations show a relatively flat nose. It is also of interest to note that Bourne noticed the plug/cone failure appearance when testing soda-lime-silica glass (see Fig. 5 from Ref. [7]). He notes that at 60 μ s, the plug begins to break up and expand radially. This trend is also noted in the HJ model of Fig 4.

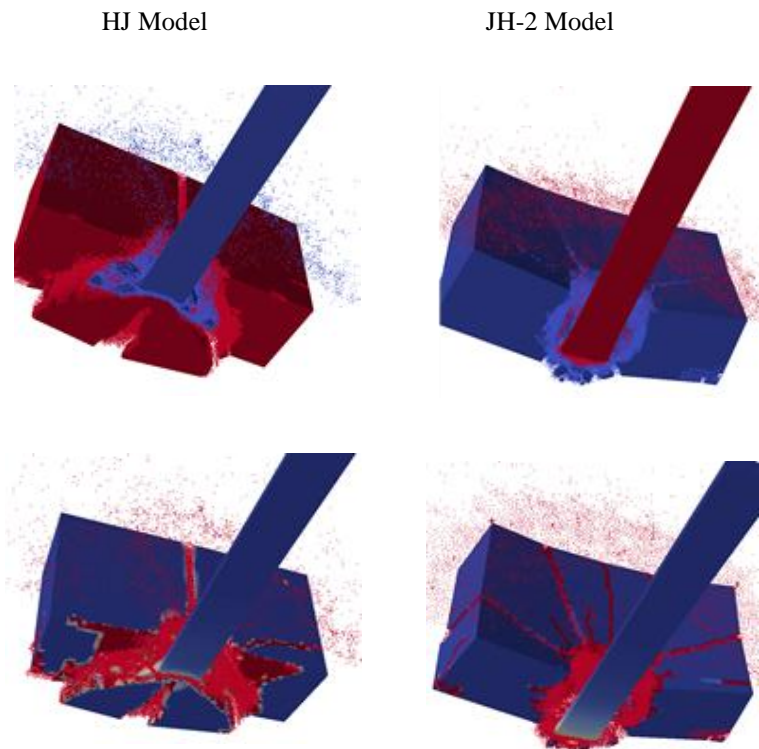


Figure 4. Three-dimensional simulation of the experiment with the HJ model and JH-2 model, colored by material (upper) and damage (lower).

Resistance to Penetration

Although the penetration rates and appearances of the two models are different, it is desirable to know the effect on the resistance of the glass block to penetration. Therefore, simulations are run with the same projectile and target, but with varying impact velocities. The strike velocity-residual velocity (V_S - V_R) data from the simulations are given in Fig. 5, along with Lamber-Jonas fit curves. The approximate limit velocities are 430 and 375 m/s for the HJ and JH-2 models, respectively. There is no experimental data to validate the computations, so the actual limit velocity of the glass block is unknown. Forde *et al.* stated an average penetration velocity of 475 m/s between 40 and 80 μ s (impact velocity of 535 to 540 m/s), which is close the JH-2 fit curve. However calculating average penetration velocities over this large range of time may not yield accurate results or correlate to residual velocity.

The overall failure of the glass is dominated by a cone of fractured and failed material. This failure mode is shown in both models (see Fig. 3) and appears to be the case for the experiment as well. As such, the simulations predict a cone of glass spall without rod penetration as low as 400 m/s and 300 m/s for the HJ and JH-2 models, respectively.

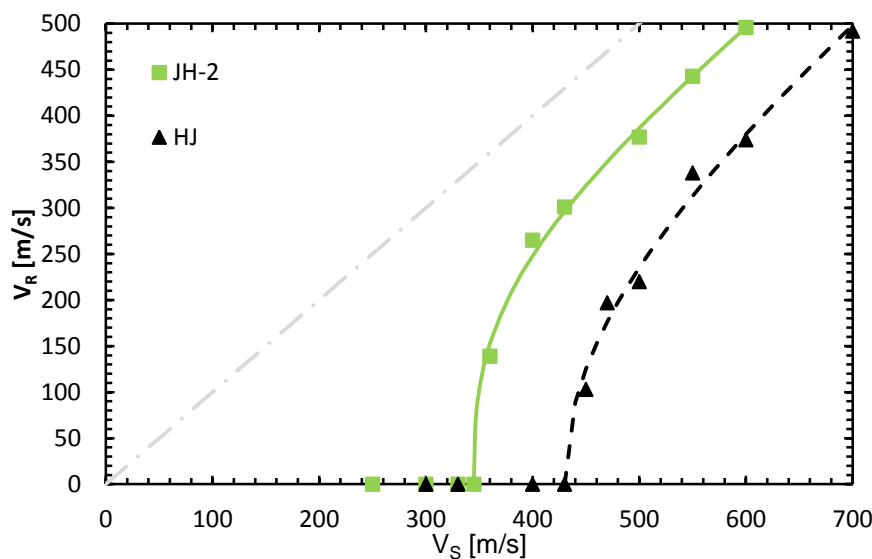


Figure 5. Residual velocity as a function of impact velocity.

Dwell-Penetration Transition

Forde *et al.* estimate that the rod dwells on the surface of the glass, however dwell may be difficult to explicitly determine based on the limited number of images available. Behner *et al.* [11] identified dwell from reverse-ballistic impact experiments using gold rods and borosilicate glass. They measured dwell until at least 32.4 μ s at an impact velocity of 412 m/s. The models in this article do not appear to predict a significant time of dwell. In these simulations, the rod initially

deforms, but there is not significant rod erosion without penetration. Significant penetration (greater than 1.5 mm) appears to begin between 10 to 15 μ s in both models. The differences in the rod material and impact velocities between the Bourne *et al.* and Behner *et al.* experiments are certainly affecting the dwell time.

Fig. 6 shows the tip and tail positions of the rod for the experiment (gray) and models relative to the undeformed glass block (blue). The rod length for the HJ model decreases substantially faster than the length for the JH-2 model. The tail positions track nearly on the same path, however the JH-2 model nose position is shown to quickly penetrate into the glass, whereas the HJ model does not penetrate as quickly. The final rod length is approximately 87 mm for the JH-2 model and 70.4 mm for the HJ model. Bourne *et al.* states a reduction in rod length due to erosion and deformation of 10 mm, which means a final length of 85 mm. This length correlates well to the JH-2 model. Note that Fig. 6 presents nose position as a negative value and the tail position as a positive value, with zero representing the strike surface of the glass block. Fig. 1 displayed the rod nose position/penetration as positive for convenience only. The nose positions reported in Figs. 1 and 5 are the same absolute value.

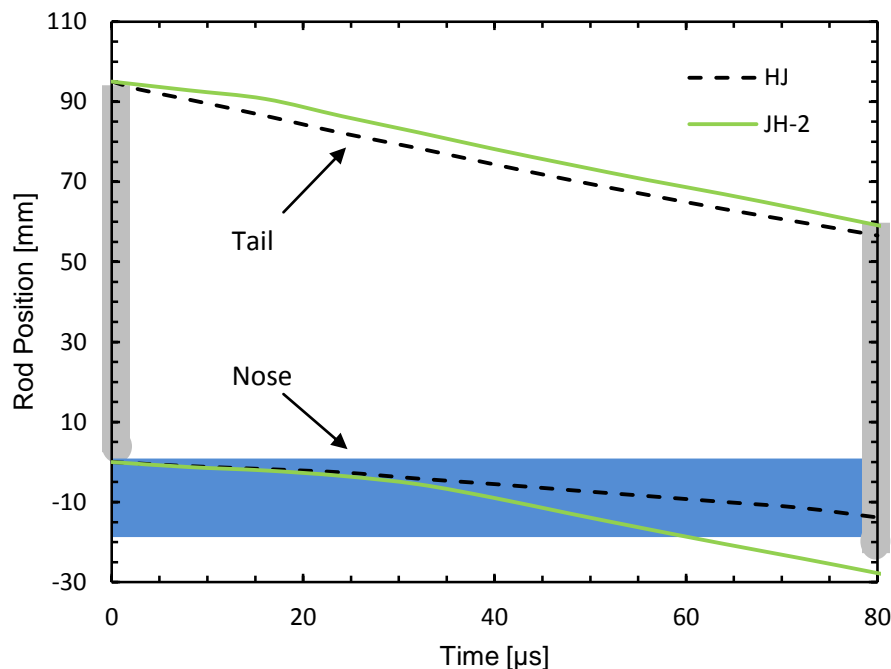


Figure 6. Nose and tail positions for the HJ and JH-2 models compared to the experimental values reported by Bourne *et al.* and the undeformed glass block.

CONCLUSION

Simulations were conducted using the Lagrangian code EPIC. The simulations compared the effects of the original Johnson-Holmquist model (JH-2) and the new Holmquist-Johnson glass model (HJ). The simulations were compared to experiments completed by Bourne *et al.* in which 9.5 x 95 mm mild steel rods were

fired at borosilicate glass blocks. The depth of penetration as a function of time, the penetration resistance, the effect of small variations in impact velocity, and the dwell-penetration transition were investigated.

The rod penetration as a function of time for the HJ model did not agree well with the experimental results, however the JH-2 model did agree well. The glass was too strong in the HJ model, however this case was seen by Refs. [1, 10].

The end quantity of concern for the practical application of a model is a performance number, such as the limit velocity. Despite the lack of experimental data to correlate to the models' limit velocity estimates, the simulations were still completed. The limit velocities differed by approximately 55 m/s, which may or not be significant. From a practical experimental stance, measuring an accurate limit velocity on brittle materials can be highly variable. The difference of 55 m/s (14.7%) may or may not be significant, depending on the experience of the researcher.

The estimated dwell time given by both models is significantly different than the 40 to 60 μ s given by Forde *et al.* and modeled by Church *et al.* [12]. The dwell time from these simulations is estimated to be between 5 to 10 μ s with significant penetration occurring between 10 to 15 μ s. One of the principles of the development of the HJ model was to reproduce dwell, therefore it is assumed that the dwell prediction should be reasonably accurate. The disagreement between the experimental and computational results may partially stem from slightly different definitions of the dwell phenomenon. (See Ref. [13] for discussion on dwell). The JH-2 model more accurately predicted the rod shortening (erosion and deformation) than the HJ model, further suggesting the overly strong glass in the HJ model. The impact velocity is not in the hydrodynamic penetration velocity regime, therefore the material strength is still important [10].

The JH-2 borosilicate glass strength constants were adjusted to maintain a similar strength profile for this impact scenario and will likely significantly over-predict the strength of the glass for high velocity impacts. This choice is a recognized shortcoming of the JH-2 approach used in this article. However, the purpose was not to compare a model in its overall state but to target the models to have similar pressure-strength relationships in this velocity regime, thereby gaining insight into the effect of the features of the model. It has previously been shown that damage propagation (which was correlated to crack propagation) in the HJ model was very sensitive changes in the location dependent strength feature in the model [10]. The thickness of the glass block in the Bourne *et al.* experiment was small relative to the rod, therefore the crack and damage propagation play a significant role in predicting the overall failure of the block, especially as the rod begins to "feel" the back surface damage of the glass. The damage contours and experimental images show cone and lateral cracking emanating from the strike face and spall-like damage beginning on the rear surface. All of these damage regions point toward a complicated state of failure. As noted by Ref [10], this complicated failure in brittle materials clouds judgment of what is right or wrong in modeling of impact and failure.

Although the HJ model depth of penetration did not correlate well to the experiment, the damage evolution mechanisms in the glass appeared to produce better visual matches to the experimental data. Material constants were not modified throughout this article, which may have produced better penetration-time

results through weakening of the glass. More experimental data for matching the location dependent strengths would provide better material constants, and therefore produce a more accurate model.

REFERENCES

1. Johnson, G.R. and Holmquist, T.J., 1994, "An Improved Computational Constitutive Model for Brittle Materials," *High Pressure Science and Technology – 1993*, S.C. Schmidt, J.W. Schaner, G.A. Samara, and M. Ross, eds., New York, pp. 981 – 984.
2. Holmquist, T.J., Johnson, G.R., Grady, D.E., Lopatin, C.M., and Hertel, E.S., 1995, "High Strain Rate Properties and Constitutive Modeling of Glass," *Proceedings of the 15th International Symposium on Ballistics*, Jerusalem, Israel.
3. Templeton, D. W. and Holmquist, T. J., 2005, "A Computational Study of Ballistic Transparencies," *Computational Ballistics 2005*. Cordoba, Spain.
4. Richards, M., Clegg, R., and Howlett, S., 1999, "Ballistic Performance of Glass Laminates Through Experimental and Numerical Investigation," *Proceedings of the 18th International Symposium on Ballistics*, San Antonio, USA.
5. Holmquist, T. J., and Johnson, G. R., 2011, "A Computational Constitutive Model for Glass Subjected to Large Strains, High Strain Rates, and High Pressures," *J. Appl. Mech.*, 78, pp. 1 – 9.
6. Bourne, N.K., Forde, L.C., Millet, J.C., and Field, J.E., 1997, "Impact and Penetration of a Borosilicate Glass," *J. Phys. IV France*, 7(C3), pp. 157 – 162.
7. Bourne, N.K., 2005. "On the Impact and Penetration of Soda-Lime Glass," *Intl. J. Impact Eng.*, 32(1-4), pp. 65 – 79.
8. Forde, L.C., Proud, W.G, Walley, S.M., Church, P.D., and Cullis, I.G., 2010, "Ballistic Impact Studies of a Borosilicate Glass," *Intl J. Impact Eng.*, 37(5), pp. 568 – 578.
9. Shockey, D., 2008, "Failure Physics of Glass during Ballistic Penetration," in *Advances in Ceramic Armor IV: Ceramic Engineering and Science Proceedings*, L.P. Franks, eds., Hoboken, pp. 23 – 32.
10. Anderson, C.E. and Holmquist, T.J., 2012, "Application of a Computational Glass Model to Compute Propagation of Failure from Ballistic Impact of Borosilicate Glass Targets," *Intl. J. Impact Eng.* Article in press.
11. Behner, Th., Anderson, C.E., Orphal, D.L., Hohler, V., Moll, M., and Templeton, D.W., 2007, "Penetration and Failure of Lead and Borosilicate Glass Against Rod Impact," *Intl. J. Impact Eng.*, 35(6), pp. 447 – 456.
12. Church, P., Goldthorpe, B., Cullis, I., and Rosenfeld, D., 2001, "Development and Validation of a Dwell Model," *Proceedings of the 19th International Symposium on Ballistics*, Interlaken, Sweden.
13. Lundberg, P., Reström, R., and Lundberg, B., 1999, "Impact of Metallic Projectiles on Ceramic Targets: Transition Between Interface Defeat and Penetration," *Intl. J. Impact Eng.*, 24(3), pp. 259 – 275.